Inorg. Chem. **2007**, *46*, 5499–5507

Acireductone Dioxygenase- (ARD-) Type Reactivity of a Nickel(II) Complex Having Monoanionic Coordination of a Model Substrate: Product Identification and Comparisons to Unreactive Analogues

Ewa Szajna-Fuller,[†] Katarzyna Rudzka,[†] Atta M. Arif,[‡] and Lisa M. Berreau*[,†]

Department of Chemistry and Biochemistry, Utah State University, Logan, Utah 84322-0300, and Department of Chemistry, University of Utah, Salt Lake City, Utah 84112

Received June 27, 2006

A mononuclear Ni(II) complex ([(6-Ph_2TPA)Ni(PhC(O)C(OH)C(O)Ph)]ClO_4 (**1**)), supported by the 6-Ph_2TPA chelate ligand (6-Ph_2TPA = *N*,*N*-bis((6-phenyl-2-pyridyl)methyl)-*N*-((2-pyridyl)methyl)amine) and containing a *cis*-β-keto-enolate ligand having a C2 hydroxyl substituent, undergoes reaction with O_2 to produce a Ni(II) monobenzoate complex ([(6-Ph_2TPA)Ni(O_2CPh)]ClO_4 (**3**)), CO, benzil (PhC(O)C(O)Ph), benzoic acid, and other minor unidentified phenyl-containing products. Complex **3** has been identified through independent synthesis and was characterized by X-ray crystallography, ^{1}H NMR, FAB-MS, FTIR, and elemental analysis. A series of *cis*-β-keto-enolate Ni(II) complexes supported by the 6-Ph_2TPA ligand ([(6-Ph_2TPA)Ni(PhC(O)CHC(O)Ph)]ClO_4 (**4**), [(6-Ph_2TPA)Ni(CH_3C-(O)CHC(O)CH_3)]ClO_4 (**5**), and [(6-Ph_2TPA)Ni(PhC(O)CHC(O)C(O)Ph) (**6**)) have been prepared and characterized. While these complexes exhibit structural and/or spectroscopic similarity to **1**, all are unreactive with O_2. The results of this study are discussed in terms of relevance to Ni(II)-containing acireductone dioxygenase enzymes, as well as in the context of recently reported cofactor-free, quercetin, and β-diketone dioxygenases.

Introduction

Acireductone dioxygenases (ARDs) are enzymes found associated with the methionine salvage pathway in species ranging from bacteria to mammals.[1−8] Two ARD enzymes having the same amino acid sequence (polypeptide chain) but which differ in the active site metal present (Fe(II) or Ni(II)) have been identified in *Klebsiella ATCC 8724*.[3] Interestingly these enzymes catalyze the oxidation of 1,2-dihydroxy-3-keto-5-(methylthio)pentene to give different products (Scheme 1). Specifically, whereas the Fe(II)−ARD catalyzed reaction yields an α-keto acid and formic acid, the Ni(II)-containing ARD enzyme instead catalyzes a shunt out of the methionine salvage pathway and the formation of a methylthiocarboxylic acid, formic acid, and CO. Results of anaerobic X-ray absorption and ^{1}H NMR spectroscopic studies of the Ni(II)−ARD from *Klebsiella ATCC 8724* suggest that a dianionic form of the substrate coordinates to the Ni(II) center in a bidentate fashion prior to reaction with O_2.[8] This notion is supported by UV−vis studies of an alternative substrate (1,2-dihydroxy-3-keto-1-hexene) and its

Scheme 1

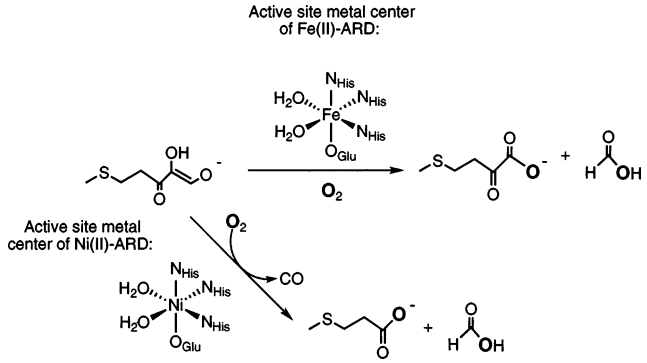

* To whom correspondence should be addressed. E-mail: berreau@cc.usu.edu. Phone: 435-797-1625. Fax: 435-797-3390.
[†] Utah State University.
[‡] University of Utah.

(1) Wray, J. W.; Abeles, R. H. *J. Biol. Chem.* **1993**, *268*, 21466−21469.
(2) Wray, J. W.; Abeles, R. H. *J. Biol. Chem.* **1995**, *270*, 3147−3153.
(3) Dai, Y.; Wensink, P. C.; Abeles, R. H. *J. Biol. Chem.* **1999**, *274*, 1193−1194.
(4) Dai, Y.; Pochapsky, T. C.; Abeles, R. H. *Biochemistry* **2001**, *40*, 6379−6387.
(5) Hirano, W.; Gotoh, I.; Uekita, T.; Seiki, M. *Genes Cells* **2005**, *20*, 565−574.
(6) Lin, T.; He, X.; Yang, L.; Shou, H.; Wu, P. *Gene* **2005**, *360*, 27−34.
(7) Oram, S.; Jiang, F.; Cai, X.; Haleem, R.; Dincer, Z.; Wang, Z. *Endocrinology* **2004**, *145*, 1933−1942.
(8) Al-Mjeni, F.; Ju, T.; Pochapsky, T. C.; Maroney, M. J. *Biochemistry* **2002**, *41*, 6761−6769.
(9) Ju, T.; Goldsmith, R. B.; Chai, S. C.; Maroney, M. J.; Pochapsky, S. S.; Pochapsky, T. C. *J. Mol. Biol.* **2006**, *393*, 823−834.

10.1021/ic061177i CCC: $37.00
Published on Web 02/13/2007

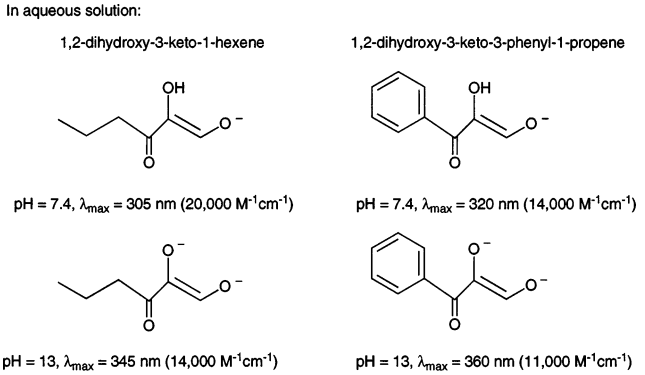

Figure 1. Protonation levels and spectroscopic properties of ARD-type substrate analogues.[4] In *Klebsiella ATCC 8724* there is one common substrate for ARD enzymes, 1,2-dihydroxy-3-keto-5-methylthiopentene. However, for mechanistic studies, where large amounts of substrate are required, substrate analogues have been used.[1]

spectroscopic properties under anaerobic conditions in the presence of Ni(II)−ARD.[4] As shown in Figure 1(left), in aqueous solution at pH = 7.4, an acireductone analogue exists as a monoanion with $\lambda_{max} = 305$ nm ($\epsilon = 20\,000$ M^{-1} cm^{-1}), whereas at pH = 13 a dianionic species is formed with $\lambda_{max} = 345$ nm ($\epsilon = 14\,000$ M^{-1} cm^{-1}).[4] In the presence of the Ni(II)−ARD enzyme at pH = 7.4, under anaerobic conditions, a $\lambda_{max} = 345$ nm is found for this substrate analogue, consistent with the formation of a dianionic species that is coordinated to the Ni(II) center.[4,8] It is worth noting that a phenyl-substituted acireductone-type substrate analogue (1,2-dihydroxy-3-oxo-3-phenyl-1-propene, Figure 1 (right)) exhibits similar behavior, with the monoanionic form having $\lambda_{max} = 320$ nm ($\epsilon = 14\,000$ M^{-1} cm^{-1}) and the dianionic form $\lambda_{max} = 360$ nm ($\epsilon = 11\,000$ M^{-1} cm^{-1}). Introduction of this substrate analogue to Ni(II)−ARD at pH = 7.4 in the absence of O_2 results in a red-shift of the absorption maximum from 320 to 360 nm. This is consistent with the formation of a coordinated dianionic species.

We recently reported the first reactive model system for Ni(II)−ARD enzymes, albeit using a bulky model substrate analogue that has not been reported to be a substrate for the enzyme.[10] Using the 6-Ph_2TPA chelate ligand, a Ni(II) *cis*-β-keto-enolate complex having a coordinated monoanionic form of the model substrate (**1**, Scheme 2) was prepared and characterized. Treatment of this complex with 1 equiv of base ($Me_4NOH{\cdot}5H_2O$) in CH_3CN under an inert atmosphere resulted in a red shift of the λ_{max} from 399 to 420 nm. This was taken as initial evidence for the formation of a new Ni(II) complex having a coordinated dianionic form of the ARD-type substrate.[11] While attempts to isolate this complex are currently in progress, we have previously shown that treatment of this dianionic substrate species with excess O_2 results in the formation of **2** and CO (Scheme 2).

In the work presented herein we have examined the reaction of **1** with O_2 in the absence of any added base. This reaction results in the formation of a mononuclear Ni(II)

Scheme 2

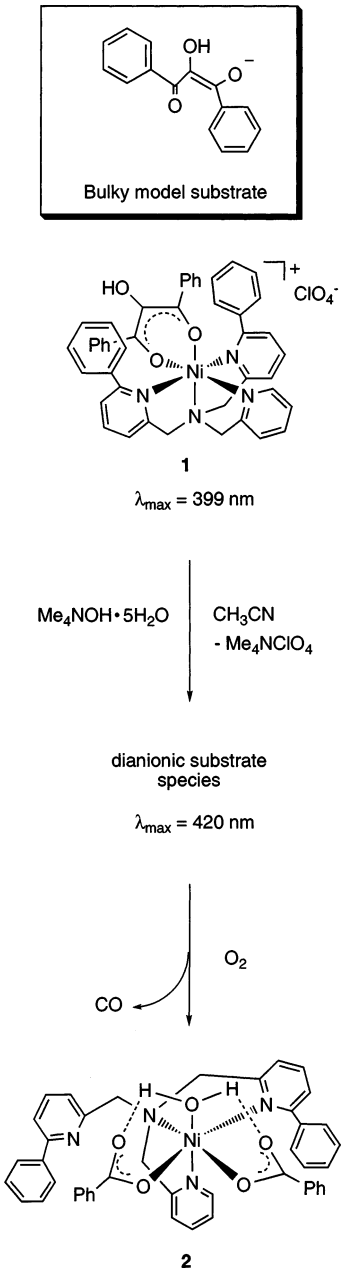

benzoate complex, CO, benzil, benzoic acid, and trace amounts of other unidentified phenyl-containing organic products. The production of CO and labeled Ni(II)-coordinated benzoate (50% ^{18}O incorporation starting from $^{18}O_2$ (99%)) in this reaction indicates that an ARD-type pathway is operative in this system. However, the production of benzil, unlabeled benzoate/benzoic acid, and other trace phenyl-containing organic products must result from an alternative reaction pathway.

In further work we have compared the structural and spectroscopic properties of **1** with those of mononuclear 6-Ph_2TPA-ligated Ni(II) complexes having a monoanionic *cis*-β-keto-enolate ligand derived from dibenzoylmethane, 2,4-pentanedione, or 1,2-dibenzoylethenol. These complexes are unreactive toward O_2.

The results of this study provide insight into factors that influence substrate reactivity in ARD type substrates and are

(10) Szajna, E.; Arif, A. M.; Berreau, L. M. *J. Am. Chem. Soc.* **2005**, *127*, 17186−17187.

(11) Significant changes occur in the ^1H NMR spectrum of **1** upon treatment with 1 equiv of $Me_4NOH{\cdot}5H_2O$.

also discussed in the context of recently reported cofactor-free, quercetin, and β-diketone dioxygenases.[12−30]

Experimental Section

General Methods. All reagents and solvents were obtained from commercial sources and were used as received unless otherwise noted. CD_3CN was dried according to a literature procedure from CaH_2 and was distilled under vacuum prior to use.[31] The 6-Ph_2-TPA ligand,[32] Ph_2TPA-d_6,[33] Ph_2TPA-d_{10},[33] and dibenzoyl-1,2-dibromoethane[34] were synthesized following literature procedures. Compound **1** was prepared as previously described.[10]

Physical Methods. ^{1}H and ^{13}C{^{1}H} NMR spectra were recorded on a JEOL GSX-270, JEOL ECX-300, or Bruker ARX-400 spectrometer. Chemical shifts (in ppm) are referenced to the residual solvent peak(s) (CD_2HCN: ^{1}H, 1.94 (quintet); ^{13}C{^{1}H}, 1.39 (heptet) ppm). ^{1}H and ^{2}H NMR spectra of paramagnetic Ni(II) complexes were acquired as previously described.[33] Longitudinal relaxation times (T_1) were measured using the inversion−recovery pulse sequence (180°−τ−90°) method. ^{1}H NMR COSY spectra for **3** and **4** were obtained in CD_3CN at 302 K and processed as previously described.[33] UV−vis spectra were recorded on a Hewlett-Packard 8453 diode array spectrophotometer. FTIR spectra were recorded on a Shimadzu FTIR-8400 spectrometer as KBr pellets. Fast atom bombardment (FAB) mass spectra were obtained at the University of California, Riverside, CA, using a VG ZAB2SE high-resolution mass spectrometer in a matrix of *m*-nitrobenzyl alcohol (MNBA). GC-MS spectra were acquired on a Shimadzu GC-MS QP5000. Elemental analyses were performed by Atlantic Microlabs of Norcross, GA. CO formation was detected using the palladium chloride method in which elemental palladium is deposited upon reaction with CO in the presence of water.[35]

Caution! *Perchlorate salts of metal salts supported by organic ligands are potentially explosive. Only small amounts of material should be prepared, and these should be handled with great care.*[36]

Treatment of [(6-Ph_2TPA)Ni(PhC(O)C(OH)C(O)Ph)]ClO_4 (1) with O_2. Identification of Products. Addition of O_2 to a CH_3CN (2 mL) solution of **1** (25 mg) at room temperature results in a rapid color change from deep orange-brown to green-yellow. Testing of an aliquot of the headspace gas using the $PdCl_2$ method[35] indicated the formation of CO during this reaction. After stirring of the solution for ∼12 h, the solvent was removed under reduced pressure. The remaining green-yellow solid was washed with Et_2O (2 × 20 mL). The Et_2O wash was then brought to dryness under reduced pressure, yielding an off-white solid. When dissolved in organic solvent, this material exhibits several overlapping resonances in the aromatic region of the ^{1}H NMR (in CD_3CN) and a GC-MS (CH_3CN) trace consistent with the presence of benzil (PhC(O)C-(O)Ph), major product), benzoic acid (minor product), and trace amounts of other unidentified phenyl-containing products. The α-keto acid benzoylformic acid is not produced. The green solid was dissolved in CH_3CN, and excess Et_2O was added, which resulted in the precipitation of a green-yellow solid. The ^{1}H NMR spectroscopic features of this solid match those of an independently generated sample of [(6-Ph_2TPA)Ni(O_2CPh)]ClO_4 (**3**).

Independent Synthesis of [(6-Ph_2TPA)Ni(O_2CPh)]ClO_4 (3). Equimolar amounts of 6-Ph_2TPA (0.025 g, 0.056 mmol) and Ni(ClO_4)$_2$·6H_2O (0.020 g, 0.056 mmol) in CH_3OH (∼2 mL) were combined with a slight excess of NaO_2CPh (0.011 g, 0.079 mmol) in CH_3OH (∼2 mL). The resulting mixture was stirred overnight at room temperature. At this point, a pale blue precipitate was present. The solvent was removed under reduced pressure, and the remaining residue was dissolved in CH_2Cl_2. This solution was filtered through a celite/glass wool plug. The filtrate was then brought to dryness under reduced pressure. A crystalline product was obtained by recrystallization of the remaining residue via diethyl ether diffusion into a CH_3CN−CH_3OH (1:2) solution at ambient temperature. This procedure yielded purple blocks suitable for single-crystal X-ray crystallography (85%). Anal. Calcd for $C_{37}H_{31}N_4O_6ClNi$: C, 61.57; H, 4.33; N, 7.76. Found: C, 61.58; H, 4.17; N, 7.77. FTIR (KBr, cm^{-1}): 1605, 1094 (ν_{ClO_4}), 621 (ν_{ClO_4}). UV−vis (CH_3CN) [nm (ϵ, M^{-1} cm^{-1})]: 395 (30), 574 (14), 1050 (15). LRFAB-MS (CH_2Cl_2/NBA) [*m*/*z* (relative intensity)]: 621 ([M − ClO_4]$^+$, 100%).

1,2-Dibenzoylethenol. A solution of NaOH (1.3 g, 30 mmol) in methanol (25 mL) was added to solid dibenzoyl-1,2-dibromoethane (0.25 g, 0.62 mmol) at room temperature, which yielded an orange reaction mixture. This solution was then stirred for 30 min at 60(1) °C. Water (25 mL) was added to the warm reaction mixture, followed by aqueous HCl (1 M) until pH ∼ 1 was reached. This resulted in the deposition of a yellow precipitate. Dichloromethane (∼150 mL) was added to the solution and precipitate, at which point the solid dissolved. The two-phase mixture was separated, and the aqueous portion was further extracted with dichloromethane (2 × ∼50 mL). The combined organic fractions were dried over

(12) Bauer, I.; Beyer de, A.; Tshisuaka, B.; Fetzner, S.; Lingens, F. *FEMS Microbiol. Lett.* **1994**, *117*, 299−304.
(13) Bauer, I.; Max, N.; Fetzner, S.; Lingens, F. *Eur. J. Biochem.* **1996**, *240*, 576−583.
(14) Frerichs-Deeken, U.; Ranguelova, K.; Kappl, R.; Hüttermann, J.; Fetzner, S. *Biochemistry* **2004**, *43*, 14485−14499.
(15) Frerichs-Deeken, U.; Fetzner, S. *Curr. Microbiol.* **2005**, *51*, 344−352.
(16) Schaab, M. R.; Barney, B. M.; Francisco, W. A. *Biochemistry* **2006**, *45*, 1009−1016.
(17) Gopal, B.; Madan, L. L.; Betz, S. F.; Kossiakoff, A. A. *Biochemistry* **2005**, *44*, 193−201.
(18) Bowater, L.; Fairhurst, S. A.; Just, V. J.; Bornemann, S. *FEBS Lett.* **2004**, *557*, 45−48.
(19) Barney, B. M.; Schaab, M. R.; LoBrutto, R.; Francisco, W. A. *Protein Expression Purif.* **2004**, *35*, 131−141.
(20) Fusetti, F.; Schröter, K. H.; Steiner, R. A.; van Noort, P. I.; Pijning, T.; Rozeboom, H. J.; Kalk, K. H.; Egmond, M. R.; Dijkstra, B. W. *Structure* **2002**, *10*, 259−268.
(21) Steiner, R. A.; Kalk, K. H.; Dijkstra, B. W. *Proc. Natl. Acad. Sci. U.S.A.* **2002**, *99*, 16625−16630.
(22) Kooter, I. M.; Steiner, R. A.; Dijkstra, B. W.; van Noort, P. I.; Egmond, M. R.; Huber, M. *Eur. J. Biochem.* **2002**, *269*, 2971−2979.
(23) Steiner, R. A.; Meyer-Klaucke, W.; Dijkstra, B. W. *Biochemistry* **2002**, *41*, 7963−7968.
(24) Steiner, R. A.; Kooter, I. M.; Dijkstra, B. W. *Biochemistry* **2002**, *41*, 7955−7962.
(25) Hund, H.-K.; Breuer, J.; Lingens, F.; Hüttermann, J.; Kappl, R.; Fetzner, S. *Eur. J. Biochem.* **1999**, *263*, 871−878.
(26) Oka, T.; Simpson, F. J. *Biochem. Biophys. Res. Commun.* **1971**, *43*, 1−5.
(27) Straganz, G. D.; Brecker, L.; Weber, H.-J.; Steiner, W.; Ribbons, D. W. *Biochem. Biophys. Res. Commun.* **2002**, *297*, 232−236.
(28) Straganz, G. D.; Glieder, A.; Brecker, L.; Ribbons, D. W.; Steiner, W. *Biochem. J.* **2003**, *369*, 573−581.
(29) Straganz, G. D.; Hofer, H.; Steiner, W.; Nidetzky, B. *J. Am. Chem. Soc.* **2004**, *126*, 12202−12203.
(30) Straganz, G. D.; Nidetzky, B. *J. Am. Chem. Soc.* **2005**, *127*, 12306−12314.
(31) Armarego, W. L. F.; Perrin, D. D. *Purification of Laboratory Chemicals*, 4th Ed.; Butterworth-Heinemann: Boston, MA, 1996.
(32) Makowska-Grzyska, M. M.; Szajna, E.; Shipley, C.; Arif, A. M.; Mitchell, M. H.; Halfen, J. A.; Berreau, L. M. *Inorg. Chem.* **2003**, *42*, 7472−7488.
(33) Szajna, E.; Dobrowolski, P.; Fuller, A. L.; Arif, A. M.; Berreau, L. M. *Inorg. Chem.* **2004**, *43*, 3988−3997.
(34) Zhang, J-J.; Schuster, G. B. *J. Am. Chem. Soc.* **1989**, *111*, 7149−7155.
(35) Allen, T. H.; Root, W. S. *J. Biol. Chem.* **1955**, *216*, 309−317.
(36) Wolsey, W. C. *J. Chem. Educ.* **1973**, *50*, A335−A337.

Na_2SO_4 and filtered, and the filtrate was brought to dryness under reduced pressure, which yielded an orange solid. This solid was recrystallized from hot ethanol, which gave the final product as an orange solid (0.11 g, 70%). This compound has been previously prepared by an alternative synthetic route, which resulted in a slightly higher yield.[37] ^{1}H NMR ($CDCl_3$, 400 MHz): δ 8.14 (d, J = 8.4 Hz, 2H), 7.99 (d, J = 8.4 Hz, 2H), 7.68−7.56 (m, 2H), 7.55−7.46 (m, 4H), 6.85 (s, 1H), hydroxyl proton not identified in wet $CDCl_3$. ^{13}C{^{1}H} NMR ($CDCl_3$, 100 MHz): δ 190.7, 187.3, 182.6, 134.5, 133.7, 130.7, 129.1, 128.9, 127.8, 96.4 (12 signals expected for inequivalent phenyl rings; 10 signals observed due to overlap of *meta*- and *para*-carbon resonances of both rings). FTIR (KBr, cm^{-1}): ∼3120 (br, ν_{OH}), 1682 (ν_{CO}), 1671 (ν_{CO}).

General Preparation Method for Ni(II) Complexes Supported by the 6-Ph$_2$TPA Ligand and Containing a Chelating Bidentate *cis*-β-Keto-Enolate Ligand. To a solution of 6-Ph$_2$TPA (0.1 mmol) in CH_3CN (∼2 mL) was added a solution of $Ni(ClO_4)_2 \cdot 6H_2O$ (0.1 mmol) in CH_3CN. The resulting mixture was stirred at ambient temperature for approximately 15 min. At this point, β-diketone (0.1 mmol) was added to the solution, followed by $Me_4NOH \cdot 5H_2O$ (0.1 mmol). This heterogeneous mixture was then stirred for 15−20 h at ambient temperature in the presence of air. The solvent was then removed under reduced pressure, and the remaining residue was dissolved in CH_2Cl_2. Filtration of this CH_2Cl_2 solution through a celite/glass wool plug enabled removal of the Me_4NClO_4 byproduct. The filtrate was then brought to dryness under reduced pressure for samples of **4** and **5**, while the solution of 6 in CH_2Cl_2 was treated with excess hexane.

[(6-Ph$_2$TPA)Ni(PhC(O)CHC(O)Ph)]ClO$_4$ (4). Recrystallized by diffusion of Et_2O into a CH_3CN-CH_3OH (1:1) solution of the complex at ambient temperature (yellow-brown microcrystals, 96%). Anal. Calcd for $C_{45}H_{37}N_4O_6ClNi$: C, 65.60; H, 4.53; N, 6.80. Found: C, 65.43; H, 4.49; N, 7.16. FTIR (KBr, cm^{-1}): 1595, 1096 (ν_{ClO_4}), 623 (ν_{ClO_4}). UV−vis (CH_3CN) [nm (ϵ, M^{-1} cm^{-1})]: 368 (13 000), 559 (14), ∼1100 (12). LRFAB-MS (CH_2Cl_2/NBA) [*m*/*z* (relative intensity)]: 723 ([M −ClO$_4$]$^+$, 100%).

[(6-Ph$_2$TPA)Ni(CH$_3$C(O)CHC(O)CH$_3$)]ClO$_4$ (5). Recrystallized from CH_3CN in the presence of excess Et_2O (X-ray-quality purple prisms, 69%). Anal. Calcd for $C_{35}H_{33}N_4O_6ClNi$: C, 60.07; H, 4.75; N, 8.01. Found: C, 59.50; H, 4.91; N, 7.73. FTIR (KBr, cm^{-1}): 1595, 1093 (ν_{ClO_4}), 622 (ν_{ClO_4}). UV−vis (CH_3CN) [nm (ϵ, M^{-1} cm^{-1})]: 238 (22 000), 285 (17 000), 548 (22), ∼1100 (14). LRFAB-MS (CH_2Cl_2/NBA) [*m*/*z* (relative intensity)]: 599 ([M − ClO$_4$]$^+$, 100%).

[(6-Ph$_2$TPA)Ni(PhC(O)CHC(O)C(O)Ph)]ClO$_4$·1.25CH$_2$Cl$_2$ (6). Following filtration in CH_2Cl_2, excess hexane was added which resulted in the deposition of yellow-orange powder (88%). Elemental analysis was performed on this powdered sample. Anal. Calcd for $C_{46}H_{37}N_4O_7ClNi \cdot 1.25CH_2Cl_2$: C, 59.23; H, 4.16; N, 5.85. Found: C, 59.28; H, 3.93; N, 5.13. X-ray-quality crystals of **6** were obtained by diffusion of pentane into a CH_2Cl_2 solution of the complex at ambient temperature. FTIR (KBr, cm^{-1}): 1675 ($\nu_{C=O}$), 1596, 1094 (ν_{ClO_4}), 622 (ν_{ClO_4}). UV−vis (CH_2Cl_2) [nm (ϵ, M^{-1} cm^{-1})]: 283 (30 000), 357 (8400). LRFAB-MS (CH_2Cl_2/NBA) [*m*/*z* (relative intensity)]: 751 ([M − ClO$_4$]$^+$, 100%).

X-ray Crystallography. A single crystal of **3**, **5**, and **6** was mounted on a glass fiber with traces of viscous oil and then transferred to a Nonius KappaCCD diffractometer with Mo Kα radiation (λ = 0.710 73 Å) for data collection at 150(1) K. An initial set of cell constants was obtained from 10 frames of data that were collected with an oscillation range of 1 deg/frame and an exposure time of 20 s/frame. Final cell constants were determined from a set of strong reflections from the actual data collection. These reflections were indexed, integrated, and corrected for Lorentz, polarization, and absorption effects using DENZO-SMN and SCALEPAC.[38] The structures were solved by a combination of direct and heavy-atom methods using SIR 97. All of the non-hydrogen atoms were refined with anisotropic displacement coefficients. Unless otherwise stated, all hydrogen atoms were assigned isotropic displacement coefficients U(H) = 1.2U(C) or 1.5U(C$_{methyl}$) and their coordinates were allowed to ride on their respective carbons using SHELXL97.[39]

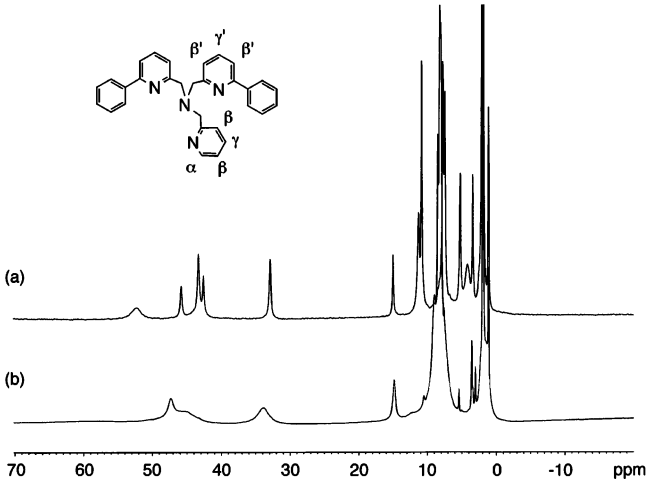

Figure 2. (a) ^{1}H NMR spectrum of **1** in CD_3CN at 25(1) °C. The sharp resonances in the region of 30−50 ppm are assigned to β/β'-H's of the pyridyl rings.[33] (b) ^{1}H NMR spectrum of **3** in CD_3CN at 25(1) °C. An identical spectrum is produced upon treatment of **1** with O_2.

Structure Solution and Refinement. Complex **3** crystallizes in the space group $P2_1/c$. All hydrogen atoms were located and independently refined. The acetylacetonate complex **5** crystallizes in the space group *Pbca*. The oxygen atoms of the perchlorate anion exhibit disorder. Each was split into two fragments, with the second being denoted by a prime, and refined. This refinement led to a 0.51:0.49 occupancy ratio. Complex **6** crystallizes in the space group $P\bar{1}$ with one molecule of methylene chloride/formula unit. All hydrogen atoms, except those of the methylene chloride solvate, were located and refined independently. Two oxygen atoms (O(6) and O(7)) of the perchlorate anion exhibit disorder. Each atom was split into two fragments, with the second being denoted by prime, and refined. This refinement led to an 81:19 ratio in occupancy.

Results

Identification of Reaction Products upon Treatment of 1 with O$_2$. Treatment of an acetonitrile solution of **1** with O_2 results in the rapid bleaching of the orange-brown color (λ_{max} = 399 nm (ϵ ∼ 6800 M^{-1} cm^{-1})) to yield a green-yellow solution (λ_{max} ∼ 570, 1050 nm). Significant changes are also evident using ^{1}H NMR (Figure 2) as a spectroscopic monitoring method. Specifically, four sharp resonances in the region of 30−50 ppm in the spectrum of **1** are replaced by a series of broad resonances. Spectroscopic studies and an independent synthesis (vide infra) confirmed the formation

(37) Lutz, R. E.; Wilder, F. N.; Parrish, C. I. *J. Am. Chem. Soc.* **1934**, *56*, 1980−1987.

(38) Otwinowski, Z.; Minor, M. *Methods Enzymol.* **1997**, *276*, 307−326.

(39) Sheldrick, G. M. *SHELXL-97, Program for the Refinement of Crystal Structures*; University of Göttingen: Göttingen, Germany, 1997.

Scheme 3

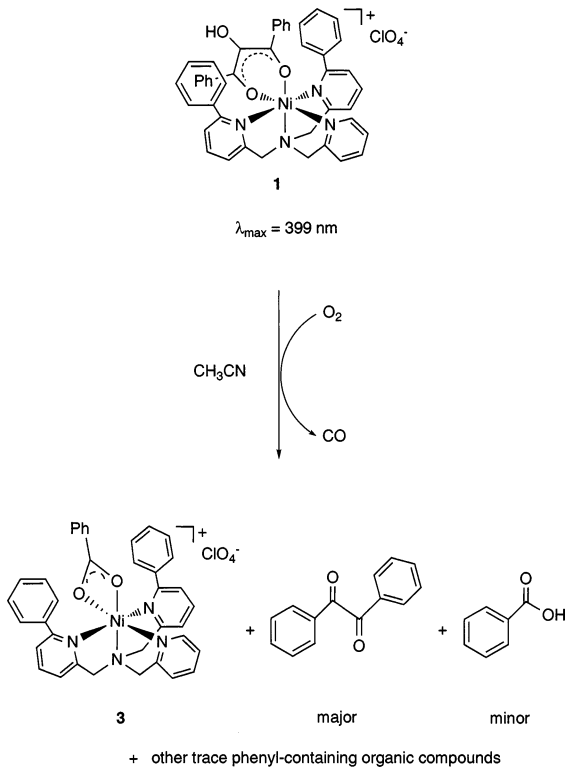

of [(6-Ph_2TPA)Ni(O_2CPh)]ClO_4 (**3**) as the only Ni(II)-containing product. Use of $^{18}O_2$ in the reaction produced **3** having ∼50% ^{18}O incorporation in the benzoate ligand. Control experiments indicate that the presence of labeled water ($H_2{}^{18}O$) in solutions of **3** does not result in the exchange of carboxylate oxygen atoms. This indicates that the 50% incorporation is not due to loss of the labeled oxygen due to exchange with adventitious water. Analysis of the headspace gas of the reaction of **1** with $^{16}O_2$ using the $PdCl_2$ method indicated the formation of CO.[35] TLC, ^{1}H NMR, and GC-MS methods were used to identify the organic products of the reaction, which were found to be benzil (major), benzoic acid (minor), and trace amounts of other unidentified phenyl-containing organic products (Scheme 3). The α-keto acid benzoylformic acid is not a product of this reaction. Quantification of the organic products was not performed at this time, as we have not yet found a method of cleanly separating the inorganic and organic products of the reaction mixture without losing some of the organic products. GC-MS analysis indicated that the benzil does not contain a labeled oxygen atom. Because the noncoordinated benzoic acid is produced in low yield, and thus far is always part of a mixture, we cannot currently report the level of ^{18}O incorporation into this product.

The Ni(II) benzoate complex **3** was identified via independent synthesis. X-ray crystallographic characterization of **3** revealed a six-coordinate Ni(II) center having bidentate[40] coordination of the benzoate ligand (Figure 3, Tables 1 and 2). The two Ni−O distances (Ni(1)−O(1) 2.0521(13), Ni(1)−O(2) 2.1293(13) Å) differ by ∼0.08 Å, with the longer being trans to the unsubstituted pyridyl donor. These distances are longer than the average Ni−O distance in **1** (∼1.97 Å) for the *cis*-*β*-keto-enolate moiety. Notably, the average Ni−N_{PhPy} distances in **1** (∼2.30 Å) and **3** (∼2.18 Å) differ considerably, with the longer average distance being found in **1** where the Ni−O bonds of the coordinated anion are shorter. From this limited **c**omparison, it appears that the Ni−N_{PhPy} bonding in these complexes is modulated depending on the interaction involving the bound anion (vide infra). In this context, it important to note that the Ni(1)−N(1) and Ni(1)−N(2) distances in **1** and **3** are generally similar (Table 2).

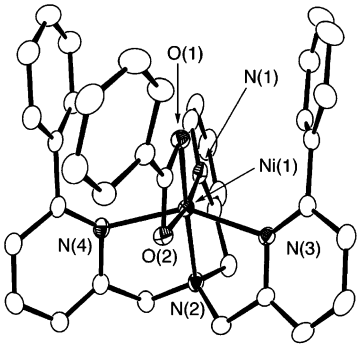

Figure 3. ORTEP representation of the cationic portion of **3**. Ellipsoids are drawn at the 50% probability level. All hydrogen atoms have been omitted for clarity.

With the identification of a number of organic byproducts for the reaction outlined in Scheme 3, we reexamined the dioxygen reactivity of **1** in the presence of 1 equiv of $Me_4NOH{\cdot}5H_2O$ (Scheme 2) to probe whether additional organic byproducts are generated in this reaction. As determined by TLC, ^{1}H NMR, and GC-MS, benzil is also produced in this reaction. However, no additional organic products are generated, thus indicating that this reaction is cleaner than the reaction involving **1** without added base (Scheme 3). This also corresponds to a higher level of ^{18}O incorporation into the benzoate product ([(6-Ph_2TPA)Ni(O_2CPh)$_2$(H_2O)], 67% ^{18}O-labeled).

Unreactive Analogues: Synthesis and Properties. We have also investigated the chemistry of Ni(II) complexes containing a *cis*-*β*-keto-enolate ligand derived from dibenzoylmethane, 2,4-pentanedione, or 1,2-dibenzoylethenol (Scheme 4, **4**−**6**). The *cis*-*β*-keto-enolate ligands in these complexes are not substrates for ARD enzymes. However, such complexes provide additional insight toward evaluating the structural and spectroscopic features of **1**. As shown in Scheme 4, these complexes (**4**−**6**) have been prepared by treatment of the 6-Ph_2TPA ligand with $Ni(ClO_4)_2{\cdot}6H_2O$, followed by addition of the *β*-diketone in the presence of 1 equiv of base. Each complex was isolated as a crystalline solid in good to high yield. Complexes **5** and **6** have been investigated using X-ray crystallography. Elemental analysis, IR, UV−vis, and mass spectrometry have also been used to characterize each complex.

X-ray crystallographic studies of **5** and **6** revealed the presence of a mononuclear six-coordinate Ni(II) center in each complex (Figure 4; Tables 1 and 2). The acetylacetonate

(40) Kleywegt, G. J.; Wiesmeijer, W. G. R.; Van Driel, G. J.; Driessen, W. L.; Reedijk, J.; Noordik, J. H. *J. Chem. Soc., Dalton Trans.* **1985**, 2177−2184.

Table 1. Summary of X-ray Data Collection and Refinement[a]

param	3	5	6
empirical formula	$C_{37}H_{31}ClN_4NiO_6$	$C_{35}H_{33}ClN_4NiO_6$	$C_{47}H_{39}Cl_3N_4NiO_7$
fw	721.82	699.81	936.88
cryst system	monoclinic	orthorhombic	triclinic
space group	$P2_1/c$	*Pbca*	$P\bar{1}$
a (Å)	10.8226(2)	18.1012(3)	11.2375(4)
b (Å)	19.9370(5)	15.7016(3)	13.4086(5)
c (Å)	15.7971(4)	22.6629(2)	16.0769(6)
α (deg)	90	90	107.4617(18)
β (deg)	103.1594(14)	90	102.107(2)
χ (deg)	90	90	103.424(3)
V (Å^3)	*3319.04(13)*	*6441.20(17)*	*2143.36(14)*
Z	4	8	2
d(calcd), Mg m^{-3}	1.445	1.443	1.452
temp (K)	150(1)	150(1)	150(1)
cryst size (mm)	0.38 × 0.20 × 0.18	0.35 × 0.35 × 0.33	0.25 × 0.15 × 0.03
diffractometer	Nonius KappaCCD	Nonius KappaCCD	Nonius KappaCCD
abs coeff (mm^{-1})	0.719	0.738	0.697
2*θ* max (deg)	54.98	54.96	50.08
completeness to 2*θ* (%)	99.5	99.8	99.4
reflcns collcd	13 079	14 018	12 473
indep reflcns	7571	7375	7516
variable params	566	464	717
R1/wR2[b]	0.0373/0.0825	0.0476/0.1204	0.0561/0.1258
goodness-of-fit (F^2)	1.019	1.014	1.043
largest diff (e Å^{-3})	0.294/−0.361	0.502/−0.620	0.956/−0.760

[a] Radiation used: Mo Kα (λ = 0.710 73 Å). [b] $R1 = \sum||F_o| - |F_c||/\sum|F_o|$; $wR2 = [\sum[w(F_o^2 - F_c^2)^2]/[\sum(F_o^2)^2]]^{1/2}$, where $w = 1/[\sigma^2(F_o^2) + (aP)^2 + bP]$.

Table 2. Selected Bond Distances (Å) and Angles (deg)[a]

param	3	5	6
Ni(1)−O(1)	2.0521(13)	2.0052(18)	1.976(2)
Ni(1)−O(2)	2.1293(13)	1.9640(16)	2.004(3)
Ni(1)−N(1)	2.0282(16)	2.051(2)	2.055(3)
Ni(1)−N(2)	2.0691(16)	2.088(2)	2.071(3)
Ni(1)−N(3)	2.1458(16)	2.217(2)	2.209(3)
Ni(1)−N(4)	2.2134(16)	2.221(2)	2.333(3)
O(1)−Ni(1)−O(2)	63.30(5)	91.56(7)	91.87(11)
O(1)−Ni(1)−N(2)	168.33(6)	94.21(8)	174.56(12)
O(2)−Ni(1)−N(2)	106.49(6)	171.69(8)	92.61(12)
N(3)−Ni(1)−N(4)	149.83(6)	150.41(8)	158.40(11)
O(2)−Ni(1)−N(1)	170.84(6)	93.30(8)	173.21(11)
O(1)−Ni(1)−N(1)	108.59(6)	174.71(8)	93.03(11)
N(1)−Ni(1)−N(3)	101.75(6)	96.52(8)	98.13(12)
N(1)−Ni(1)−N(4)	97.48(6)	99.05(8)	79.62(12)
N(1)−Ni(1)−N(2)	81.99(7)	81.19(8)	82.77(12)
N(2)−Ni(1)−N(3)	77.80(6)	81.70(8)	78.15(11)
N(2)−NI(1)−N(4)	82.16(6)	76.05(8)	80.26(11)

[a] Estimated standard deviations in the last significant figure are given in parentheses.

derivative **5** exhibits a shorter average Ni(1)−N_{PhPy} distance (2.22 Å) than **1** and **6** (2.30 and 2.27 Å, respectively). Thus, the N_{PhPy} distance is longer in complexes having a bulkier *cis*-*β*-keto-enolate ligand. The Ni(1)−N(1) and Ni(1)−N(2) distances associated with the pyridyl and tertiary amine donors of the 6-Ph_2TPA ligand exhibit only minimal differences (<0.025 Å) in this series of complexes. Similarly, the average Ni−O distance involving the *cis*-*β*-keto-enolate ligand shows little variability (1.96−1.99 Å). Therefore, the overall coordination environments of the Ni(II) centers in **1**, **5**, and **6** are similar, with subtle perturbation of the average Ni(1)−N_{PhPy} distance as a function of *cis*-*β*-keto-enolate ligand.

The IR spectra of **4**−**6** are generally similar and all contain the vibrations expected for the noncoordinated tetrahedral

Scheme 4

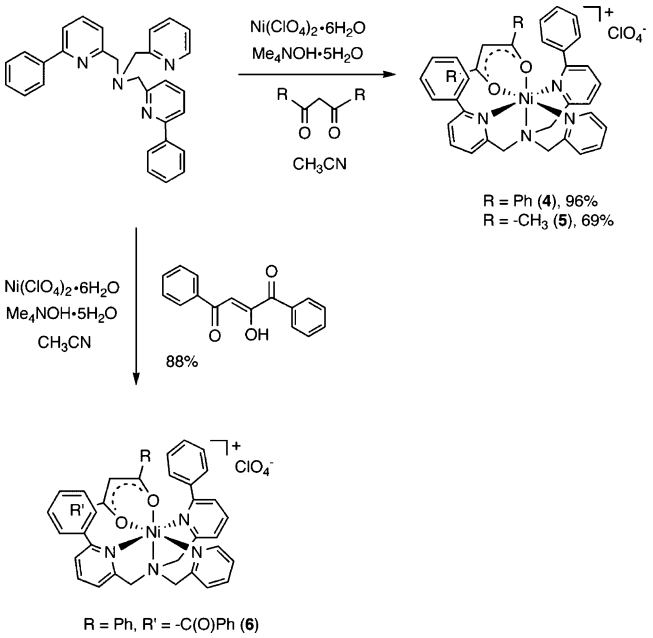

perchlorate anion (∼1095 and 625 cm^{-1}).[41] The infrared spectrum of **6** also contains a vibration at 1675 cm^{-1} consistent with the presence of a noncoordinated ketone carbonyl group.[42]

The UV−vis spectra of **4** and **6** contain an intense absorption feature at 368 and 357 nm (Table 3), respectively. These features are at higher energy and exhibit stronger intensities than a similar absorption band present in the spectrum of **1** at 399 nm. These absorptions are tentatively

(41) Nakamoto, K. *Infrared and Raman Spectra of Inorganic and Coordination Compounds*, 5th ed.; Wiley & Sons: New York, 1997.
(42) Silverstein, R. M.; Webster, F. X. *Spectrometric Identification of Organic Compounds*, 6th ed.; Wiley & Sons: New York, 1998.

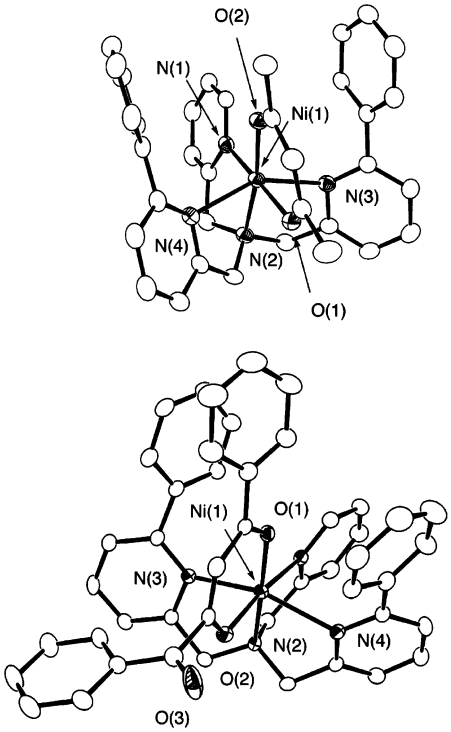

Figure 4. ORTEP representations of the cationic portions of **5** and **6**. Ellipsoids are drawn at the 35% probability level. All hydrogen atoms have been omitted for clarity.

Table 3. $\pi \rightarrow \pi^*$ Transitions of Ni(II) Complexes Having an Aryl-Containing *cis*-β-Keto-Enolate Ligand (in CH_3CN)

anion or complex	λ_{max} (ϵ, $M^{-1}\,cm^{-1}$)
1	399 (6800)
4	368 (13 000)
6	357 (8400)

assigned as being derived from an intraligand $\pi \rightarrow \pi^*$ transition (Table 3) in the *cis*-β-keto-enolate ligand.[43,44] It is worth noting that Na(PhC(O)CHC(O)Ph) and Me_4N(PhC(O)CHC(O)C(O)Ph) exhibit a $\pi \rightarrow \pi^*$ transition at 352 and 335 nm in CH_3CN solution, respectively.[43]

Consistent with the solid-state structural similarities outlined above for **1**, **5**, and **6**, the ^{1}H NMR features of these complexes are highly similar (Figure 5), albeit a resonance upfield of 0 ppm is present in **4**−**6**. This resonance, which has been definitively assigned using acetylacetone-d_2 as a precursor for the preparation of [(6-Ph_2TPA)Ni(CH_3C(O)CDC(O)CH_3)]ClO_4 (**4**-d_1), is assigned to the proton on the *cis*-β-keto-enolate moiety. In **1** the hydroxyl group replaces this proton. The four relatively sharp resonances in the range of 30−50 ppm for **1** and **4**−**6** are assigned to the β/β'-H's (inset, Figure 2) of the pyridyl rings of 6-Ph_2TPA on the basis of chemical shift, T_1 values, relative integration, and comparison with the spectra of previously reported Ni(II) complexes supported by this chelate ligand.[33] The identification of a total of four pyridyl β/β' proton resonances is consistent with an effective plane of symmetry in these complexes which yields spectroscopically equivalent phenyl-

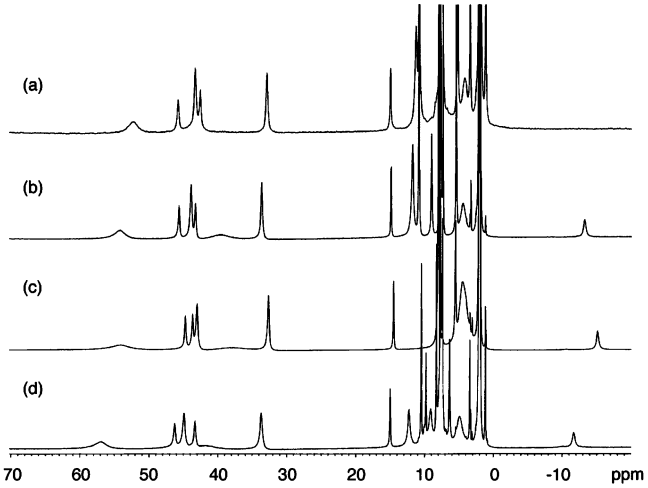

Figure 5. ^{1}H NMR spectra of mononuclear Ni(II) *cis*-β-keto-enolate complexes in CD_3CN at 25(1) °C: (a) [(6-Ph_2TPA)Ni(PhC(O)C(OH)C(O)Ph)]ClO_4 (**1**); (b) [(6-Ph_2TPA)Ni(PhC(O)CHC(O)Ph)]ClO_4 (**4**); (c) [(6-Ph_2TPA)Ni(CH_3C(O)CHC(O)CH_3)]ClO_4 (**5**); (d) [(6-Ph_2TPA)Ni(PhC(O)CHC(O)C(O)Ph)]ClO_4 (**6**).

appended pyridyl donors. This plane of symmetry is evident in the X-ray structures of **1**, **5**, and **6** wherein the bound *cis*-β-keto-enolate ligand is positioned in a sandwich-type motif between the two phenyl-appended pyridyl groups. The β/β' proton resonances were assigned to either pyridyl ring protons or phenyl pyridyl ring protons on the basis of integration. For example, in the spectrum of **4** (Figure 5b), the signal at 34.1 ppm integrates to two protons relative to the integration of the upfield-shifted *cis*-β-keto-enolate proton resonance at −13.3 ppm. This signal is assigned as a β' proton resonance of the phenyl-appended pyridyl rings (Figure 2 (inset)). A resonance of similar intensity is found at 44.6 ppm, albeit it cannot individually be integrated due to overlap with another resonance. The two resonances at 46.3 and 43.8 ppm are assigned as the β-H resonances of the unsubstituted pyridyl donor. The larger downfield shift for the β' (phenyl pyridyl) resonances relative to the β (pyridyl) proton resonances is consistent with differences in the ligand field and spin distribution for these two different types of donors. The phenyl-appended pyridyl donors have longer Ni−N distances than the pyridyl appendage. As the hyperfine shifts of the resonances in these types of complexes have a significant contact contribution,[33] the protons of the unsubstituted pyridyl ring, which are closer to the paramagnetic Ni(II) center, exhibit a slightly greater hyperfine shift. A similar description is appropriate for the spectral features of **1**, **5**, and **6** in the region of 30−50 ppm.

Discussion

The results outlined herein, together with our previously reported studies,[10] indicate that Ni(II)−ARD-type products (carboxylates and CO) are generated in the reaction of O_2 with a Ni(II) complex having a bulky ARD model substrate coordinated as a monoanion or dianion. The formation of **3** in the reaction of **1** with O_2 requires the production of one equivalent of benzoate. If this reaction were going exclusively by an ARD-type pathway, CO generation would be accompanied by the production of 2 equiv of benzoate/benzoic

(43) Halcrow, M. A.; Sun, J.-S.; Huffman, J. C.; Christou, G. *Inorg. Chem.* **1995**, *34*, 4167−4177.
(44) Eistert, B.; Weygand, F.; Csendes, E. *Chem. Ber.* **1951**, *84*, 745−780.

acid and a high level of ^{18}O incorporation would be expected.[2] On the basis of our identification of the production of CO and 1 equiv of benzoate in **3** (with only 50% ^{18}O incorporation), we propose that only a portion of the benzoate (~50%) is coming from an ARD-type reaction. The benzil, unlabeled benzoate, benzoic acid, and other phenyl-containing products must be coming from an alternative reaction pathway(s). This pathway may involve the generation of benzoyl radicals, which could be the precursor to benzil formation.[45] Notably, the radical decomposition of α-hydroperoxy ketones has been demonstrated to produce benzoyl radicals (e.g., $PhC(O)^{\bullet}$) and benzoic acid. We also note that the dianionic species formed by treatment of **1** with 1 equiv of $Me_4NOH{\cdot}5H_2O$ in CH_3CN exhibits a cleaner reaction with O_2. Specifically, while benzil is generated, the benzoate ligands in **2** (which is isolated in 75% yield as a crystalline solid) contain ~67% ^{18}O incorporation.

The reaction of the Ni(II)-coordinated monoanion $PhC(O)C(OH)C(O)Ph^-$ with O_2 has some precedent in the chemical literature, as carbanions have been shown to react with oxygen to form peroxide anions.[46−48] These reactions may occur by a single electron transfer (SET) process,[49] which would result in the generation of an organic radical and superoxide, or via a two-electron step between the anionic substrate and electrophilic O_2. Studies of the reactivity of Ni(II)−ARD suggest that a radical reaction may be occurring in the enzyme-catalyzed reaction, albeit from a Ni(II)-coordinated dianionic form of the substrate.[4] The evidence for this radical chemistry comes from studies involving a cyclopropyl-containing substrate analogue. The enzyme/substrate complex formed using this analogue is not EPR active, indicating that no radical is present. However, in the presence of O_2 the cyclopropyl-containing substrate analogue slowly and irreversibly inhibits Ni(II)−ARD after ~100 turnovers, suggesting that radical chemistry may be occurring.[4] Involvement of a radical pathway is also supported by recent computational studies.[50]

CO-producing reactions similar to that catalyzed by Ni(II)−ARD are catalyzed by the cofactor-free 1*H*-3-hydroxy-4-oxoquinaldine 2,4-dioxygenase and by quercetin dioxygenase.[12−26] The former cofactor-free enzyme has been shown to catalyze the reaction of the substrate dianion with O_2 to form a resonance-stabilized radical anion.[14] Specifically, in the ternary complex (enzyme/substrate/O_2) single electron transfer occurs from the substrate dianion to O_2, resulting in the formation of a radical pair (Scheme 5). Radical recombination is proposed to yield a peroxide species that then proceeds via intramolecular attack to yield the reaction products.

In quercetin dioxygenase enzymes, the flavonol-type substrate binds to a metal center (either Cu(II), Fe(II), or Mn(II)) as a monoanion via the hydroxyl moiety in the substrate.[20−24] This monoanion may take on radical character via internal redox involving the metal center (e.g., Cu(II)). This radical can then undergo reaction with O_2 to yield a reactive peroxide moiety. Alternative mechanistic pathways have been proposed wherein the presence of a reduced metal center may also participate in oxygen activation via formation of a metal−superoxide species.[16−19] Quercetin and other flavonol-type substrates are also reactive with O_2 in the absence of metal ions under basic conditions.[51−54] This type of reaction yields the same types of products (a phenolic carboxylic acid ester and CO, Scheme 6) as those produced by quercetin dioxygenase enzymes. In DMF, reaction between potassium flavonolate and O_2 proceeds by a single-electron-transfer mechanism (SET) as evidenced by the identification of a flavonoxyl radical by EPR.[49,52] In 50% DMSO−H_2O solution at pH = 6.4−10.8 the same reaction is suggested to proceed via direct reaction of the deprotonated flavonol and O_2 in a two-electron step.[53] Thus, depending

Scheme 5

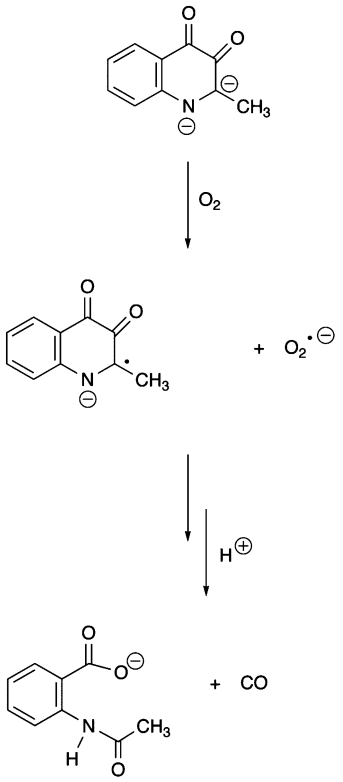

Scheme 6

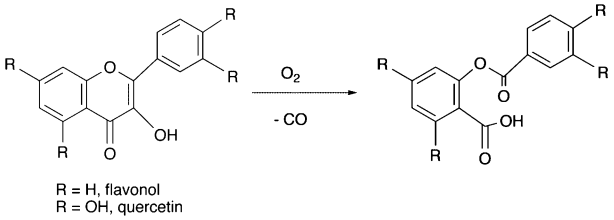

(45) Sawaki, Y.; Ogata, Y. *J. Org. Chem.* **1976**, *41*, 2340−2343.
(46) Barton, D. H. R.; Jones, D. W. *J. Chem. Soc.* **1965**, 3563−3570.
(47) Gersmann, H. R.; Bickel, A. F. *J. Chem. Soc., B* **1971**, 2230−2237.
(48) Abell, L. M.; Schloss, J. V. *Biochemistry* **1991**, *30*, 7883−7887.
(49) Smith, M. B.; March, J. *Advanced Organic Chemistry*, 5th ed.; Wiley-Interscience: New York, 2001; pp 402−404.
(50) Borowski, T.; Bassan, A.; Siegbahn, P. E. M. *J. Mol. Struct.* **2006**, *772*, 89−92.
(51) Nishinaga, A.; Tojo, T.; Tomita, H.; Matsuura, T. *J. Chem. Soc., Perkin Trans. 1* **1979**, 2511−2516.
(52) Rajananda, V.; Brown, S. B. *Tetrahedron Lett.* **1981**, *22*, 4331−4334.
(53) Barhács, L.; Kaizer, J.; Speier, G. *J. Org. Chem.* **2000**, *65*, 3449−3452.
(54) Balogh-Hergovich, E.; Speier, G. *J. Org. Chem.* **2001**, *66*, 7974−7978.

on conditions, it appears that this reaction can proceed via two reaction pathways.

The role of the Ni(II) ion in Ni(II)−ARD may be to act as a Lewis acid to ensure formation of a dianionic form of the substrate. As noted in the Introduction, there is spectroscopic evidence in support of the formation of an enzyme/substrate adduct in Ni(II)−ARD wherein the substrate is coordinated to Ni(II) as a dianion prior to reaction with O_2.[8] For nonenzymatic reactions involving the model substrate 1,2-dihydroxy-3-oxo-hexene (Scheme 1), the rate of reaction between the substrate dianion (at pH = 13) and O_2 is approximately 66× faster than the reaction involving the substrate monoanion (at pH = 7.5).[4] Formation of a Ni(II)-coordinated substrate dianion may be essential to producing an appropriate rate of reaction involving O_2. On the basis of the results presented herein, formation of a Ni(II)-coordinated dianionic species may also be important toward limiting alternative oxidation pathways.

The preparation and characterization of **4**−**6** has enabled an examination of how the structural and electronic properties of the Ni(II) center are influenced by changes in the *cis*-β-keto-enolate monoanion. The UV−vis spectra of **1** and **4** exhibit differences in terms of the energy and molar absorptivity of the $\pi \rightarrow \pi^*$ transition (Table 3). The lower energy of the $\pi \rightarrow \pi^*$ transition in **1** indicates either destabilization of the π orbitals or stabilization of the π^* orbital due to the presence of the hydroxyl substitutent. The reactive nature of **1** toward O_2 correlates with the presence of the hydroxyl group, as **4** is unreactive with O_2. The similarity of the ^{1}H NMR spectral features of **1** and **4**−**6** (Table 4) suggests similar unpaired spin delocalization properties in this family of complexes.

With regard to the O_2 reaction of metal-bound *cis*-β-keto-enolate ligands, it is worth noting that a non-heme iron dioxygenase was recently reported which catalyzes the O_2-dependent oxidative aliphatic carbon−carbon bond cleavage of acetylacetone into methylglyoxal and acetate.[27−30] This enzyme, termed diketone dioxygenase (Dke1), was obtained from a strain of *Acinetobacter johnsonii* and requires Fe(II) for activity. Replacement of Fe(II) with other metal ions, including Ni(II), yields inactive enzyme. A mechanistic pathway for acetylacetone oxidation has been proposed wherein the substrate binds to the Fe(II) center as a bidentate monoanionic *cis*-β-keto-enolate ligand. The Fe(II) center is proposed to couple the oxidation of the bound substrate with dioxygen reduction. An important feature of the Dke1 active site is the presence of only three amino acid ligands (all histidines) bound to the Fe(II) center. In the presence of the bidentate coordinated substrate, this leaves one metal coordination site available for interaction with O_2, which may be required for the oxidation of *cis*-β-keto-enolate-type substrates that lack a C2-hydroxyl moiety.

Table 4. Assignment of Selected ^{1}H NMR Resonances of **1** and **4**[a]

assgnt	chem shift (ppm)[b]	$\Delta\nu_{1.2}$ (Hz)[c]	T_{1exp} (ms)[d]	rel area
	[(6-Ph$_2$TPA)Ni(PhC(O)C(OH)C(O)Ph)]ClO$_4$ (**1**)			
β	45.8, 42.6	100, 80	6, 7	1, 1
β	43.3, 32.9	120, 110	7, 5	2, 2
γ	15.0	42	21	1
γ	5.2	64	17	2
	[(6-Ph$_2$TPA)Ni(PhC(O)CHC(O)Ph)]ClO$_4$ (**4**)			
β	46.3, 43.8	82, 69	6, 8	1, 1
β	44.6, 34.1	100, 86	6, 4	2, 2
γ	15.0	33	18	1
γ	5.4	40	15	2
CH	−13.3	140	3	1

[a] The ^{1}H NMR features of **5** and **6** are similar to those exhibited by **4** (see Figure 5). [b] Chemical shifts in ppm relative to the residual solvent peak of C*H*D$_2$CN (^{1}H, 1.94 (quintet) ppm). [c] Line widths are full width at half-maximum. [d] T_1 values were obtained at 300 MHz.

Acknowledgment. We thank the National Institutes of Health (Grant 1R15GM072509) for financial support of this work and Sara Huefner for technical assistance.

Supporting Information Available: X-ray crystallographic (CIF) files for **3**, **5**, and **6**. This material is available free of charge via the Internet at http://pubs.acs.org.

IC061177I